Impurity transport studies using fast imaging of injected carbon on the MAST tokamak

H.J. Leggate[1], S.W. Lisgo[2], J.R. Harrison[3], S.A. Silburn[4], S Elmore[3], S.Y. Allan[3], M.M. Turner[1]

[1] *National Centre for Plasma Science and Technology, Dublin City University, Dublin, Ireland*

[2] *ITER Organisation, Route de Vinon, CS 90 046 13067 Saint Paul Lez Durance, France*

[3] *Culham Centre for Fusion Energy, Culham Science Centre, Abingdon, Oxon OX14 3DB, UK*

[4] *The University of Durham, The Palatine Centre, Stockton Rd, Durham, DH1 3LE, UK*

The operation of next-generation fusion reactors will be significantly affected by impurity transport in the scrape-off layer (SOL). Current modelling efforts are restricted by a lack of detailed data on impurity transport in the SOL. The Spark Gap Impurity Injector previously installed on the MAST tokamak injects small quantities of carbon close to the lower outer strike point. The injector was re-installed on the Divertor Science Facility during 2013 after modification of the power supplies to allow for operation during beam heated plasmas. Carbon was injected into single beam heated L-mode discharges and two beam heated H-mode discharges. The carbon plume created by the the injector was imaged using 2 fast cameras filtered to the carbon II(514nm) and carbon III(465nm) emission lines and operated at 75kHz - 100kHz. Strong carbon II emission was seen in all shots but no significant carbon III emission was observed upstream from the injection location for either the L-mode or H-mode shots. The plumes give a measurement of the transport of carbon ions which is then compared to simulation using the OSM-EIRENE-DIVIMP codes.

Introduction

The transport of impurities in the plasma Scrape-Off Layer (SOL) is of vital importance to the performance of existing and future magnetic confinement fusion devices. The impurities play a major role in both the heat loads to the plasma facing components and the performance of the core plasma. An understanding of the impurity transport is required in order to calculate the influx of impurities to the confined plasma which arise due to chemical and physical sputtering of plasma facing components and impurity seeding. The injection of impurities into fusion plasmas as a diagnostic of transport has been performed using a variety of methods (1; 2). Detailed studies using edge impurity injection have not previously been carried out on a spherical tokamak and the advanced diagnostic capabilities available on the MAST tokamak mean that the technique is ideally suited to this machine. The new method described here uses an electrical discharge to inject carbon in the MAST divertor.

Injector design and installation

The Spark Gap Impurity Injector was first installed and commissioned on the MAST Divertor Science Facility (3) during the 2011 experimental campaign. The injector operates by creating an electrical discharge between a pair of concentric cylindrical carbon electrodes. This ablates approximately 10^{15} carbon atoms as both ions and neutrals into the MAST divertor on a timescale of approximately $10\mu s$. A schematic cross-section of the head design can be seen in figure 1. An arc is formed by discharging a $1.5\mu F$ capacitor bank that can be charged to a maximum of 2.5kV across the electrodes. A Langmuir probe is also incorporated into the injector head to provide local density and temperature measurements.

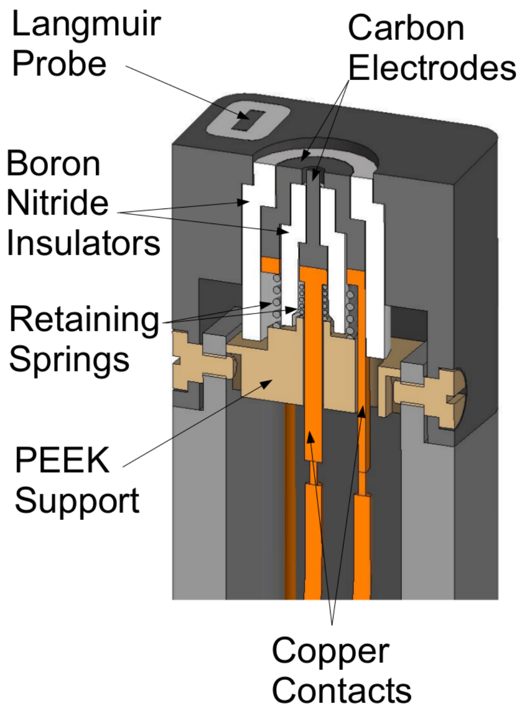

Figure 1: Schematic of the injector head.

Experimental results and analysis

The injector was re-installed during the 2013 experimental campaign and carbon was injected into beam heated L-mode and H-mode shots. The L-mode shots were operated with plasma conditions $I_p \approx 900MA$, $B_T \approx 0.55T$, $n_e \approx 1.6 \times 10^{19} m^{-3}$ and $P_{NBI} \approx 1.8MW$ and the H-mode shots with $I_p \approx 900MA$, $B_T \approx 0.55T$, $n_e \approx 3 \times 10^{19} m^{-3}$ and $P_{NBI} \approx 3.5MW$. The plumes created were imaged from 2 toroidal locations using fast cameras operating at $75kHz$ - $100kHz$ and filtered to the CII and CIII emission lines. Plasma flow measurements were taken using coherence imaging (4).

The plasma conditions vary significantly with radial position relative to the lower outer strike-point. It is therefore important to identify the position of the strike-point as accurately as possible. This was determined using EFIT equilibrium reconstruction, the divertor Langmuir probes and the Langmuir probe incorporated into the injector head. Figure 2 shows the electron density radially across the divertor for 3 shots, 29125, 29126 and 21939 measured using the divertor Langmuir probes. The plots show data at the three times closest to the injection time, during which the strike-point can be assumed to be stationary to an accuracy of 1mm. For the 2 L-mode shots 29125 and 29126 the injection location can be seen to be at the strike-point and 2cm outside the strike-point and for the H-mode shot the injection occurred 2-3cm outside the strike-point.

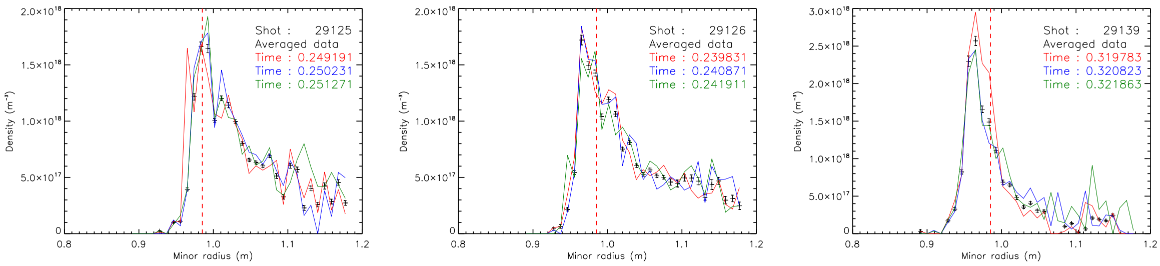

(a) L-mode on the strike-point (b) L-mode 2cm from strike-point (c) H-mode 3cm from strike-point

Figure 2: Electron density data from the divertor Langmuir probes showing the location of the outer strike-point for each shot. The red dashed line shows the injection location.

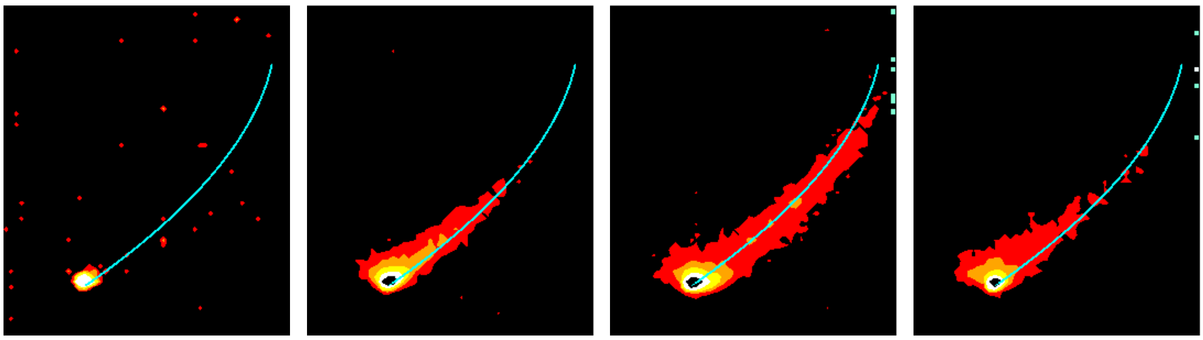

(a) $13\mu s$ (b) $26\mu s$ (c) $40\mu s$ (d) $53\mu s$

Figure 3: The projection of the field line (coloured cyan) originating at the injection location can be seen plotted over contour plots of the CII emission for consecutive frames from the sector 1 camera during the H-mode shot 29139 operating at $75kHz$. The displayed times refer to the end of each frame relative to the start of the first frame. For perspective the field line trace corresponds to $0.5m$ along the field line.

The extent of the observed plumes parallel to the magnetic field was calculated from the camera images. The field lines were followed using data from the EFIT equilibrium reconstruction code and then projected onto the images of the expanding plume. Figures 3 and 4 show the projection of field lines and the corresponding intensity along the field line for three consecutive frames from the H-mode shot 29139. From this data the parallel speed of the plume expansion is calculated to be $14 \pm 3kms^{-1}$ compared to the local sound speed $c_s \approx 30kms^{-1}$.

DIVIMP modelling

The injection of singly ionized carbon into the MAST divertor was simulated using the 2D Monte-Carlo code DIVIMP (5). DIVIMP follows impurities on a hydrogenic background generated using the OSM (6) onion skin model with neutral effects included by using EIRENE (7). OSM relies on a detailed specification of the experimental conditions. The electron temperature and density at the mid-plane and targets is specified using Langmuir probe and Thomson scattering data and $T_i = T_e$ see (8). A recent extension to DIVIMP allows the simulation of ion

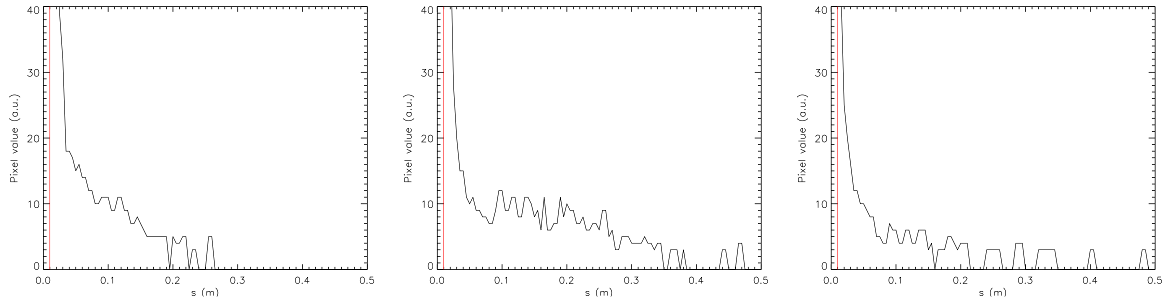

(a) 26μs (b) 40μs (c) 53μs

Figure 4: Measured intensity projected onto the originating field line for three successive frames for H-mode pulse 29139 corresponding to the field lines traced in figure 3, the vertical red line shows the injection location.

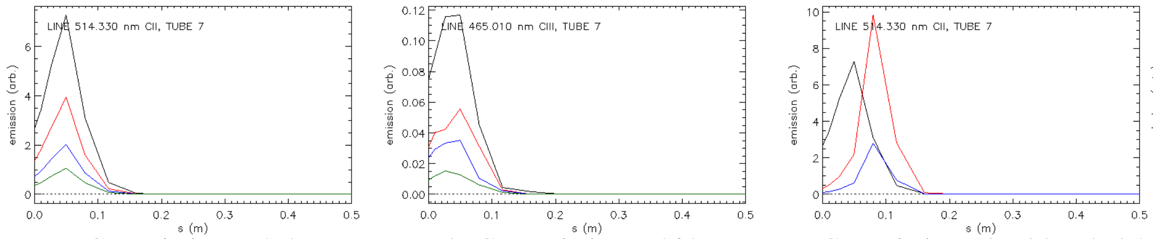

(a) CII emission at 514nm (b) CIII emission at 465nm (c) CII emission, 13, 104 and 195μs

Figure 5: Simulated carbon II (a) and carbon III (b) emission along the field line originating from the injection location at times corresponding to the frames in figure 3. Each time is overlaid on the same plot with order black, red, blue green. Plot c shows emission after 13μs 104μs and 195μs showing the slow movement of the plume calculated by DIVIMP.

injection for a finite time with the injected ions followed during and after the injection, replicating the experimental scenario. Previous DIVIMP versions required an injected source to be active during the entire simulation. The parallel extent of injected carbon from these preliminary simulations at times corresponding to those in the camera images can be seen in figure 5. It can be seen that DIVIMP does not show the fast expansion along the field line seen in experiment, further work is required to identify the reasons behind this discrepancy.

This work was part-funded by the RCUK Energy Programme [grant number EP/I501045] and by the European Union's Horizon 2020 research and innovation programme. The views and opinions expressed herein do not necessarily reflect those of the European Commission.

References

[1] C. Giroud, R. Barnsley, P. Buratti, et al. *Nucl Fusion*, 47:313–330, 2007.
[2] S. Gangadhara and B. LaBombard. *Plasma Phys Contr F*, 313-316:1167–1172, 2003.
[3] G. De Temmerman, M. Bacharis, J. Dowling, and S. Lisgo. *Nucl Fusion*, 50:105012, 2010.
[4] S.A. Silburn, R.M. Sharples, C.A. Michael, et al. In *Plasma Physics, Europhysics Conference Abstracts, European Physical Society, 2013*, volume 37D, page P6.019, 2014.
[5] P.C. Stangeby and J.D. Elder. *Nucl Fusion*, 35(11):1391–1412, 1995.
[6] S. Lisgo et al. *J Nucl Mater*, 337-339:139–145, 2005.
[7] D. Reiter. *J Nucl Mater*, 196-198:80–89, 1992.
[8] S. Elmore, S Y Allan, A Kirk, et al. *Plasma Phys Contr F*, 54:065001, 2012.